ORIGINAL ARTICLE

Veterinary Research Forum. 2024; 15 (11): 629 - 643
doi: 10.30466/vrf.2024.2022533.4165
Journal Homepage: vrf.iranjournals.ir

Veterinary Research Forum

MicroRNA-142-3p chemo-sensitizing breast cancer to docetaxel: apoptosis and cell cycle arrest induction, and migration suppression

Masoumeh Moradi Ozarlou[1]*, Razeieh Dehghan[1], Behzad Mansoori[2,3], Behzad Baradaran[2]

[1] Department of Pathobiology, Faculty of Veterinary Medicine, University of Tabriz, Tabriz, Iran; [2] Immunology Research Center, Tabriz University of Medical Sciences, Tabriz, Iran; [3] Department of Cancer and Inflammation Research, Institute for Molecular Medicine, University of Southern Denmark, Odense, Denmark.

Article Info

Article history:

Received: 08 February 2024
Accepted: 29 June 2024
Available online: 15 November 2024

Keywords:

Breast cancer
Cancer therapy
Chemotherapy
Docetaxel
MicroRNA-142-3p

Abstract

Docetaxel (DTX) is widely utilized in breast cancer treatment. However, cancer cell resistance has limited its anti-tumor efficacy. Some molecules called microRNAs (miRNAs), acting like fine-tuned switches, can influence how breast cancer develops and spreads. We conducted a study to examine if augmenting breast cancer cells with a particular molecule, known as miRNA-142-3p, could improve the efficacy of a widely used treatment called DTX. The expression level of miR-142-3p was initially assessed in MDA-MB-468 cells. The miRNA transfection was performed to conduct additional experiments. The impact of a combined treatment involving DTX and miRNA-142-3p on both cell migration (by wound healing assay) and apoptosis (using annexin V/Propidium iodide staining) was examined. Cell viability was determined through the MTT assay, and gene expression was quantified using quantitative real-time polymerase chain reaction. The combined application of DTX and miRNA-142-3p resulted in a significant decrease in the expression of factors promoting tumor growth, such as SOX2, Octamer 4, HMGA2, Kruppel-like factor 4, and Bach-1. Additionally, the combination of miRNA-142-3p and DTX initiated apoptotic cell death. Moreover, the progression of breast cancer cells was impeded by inducing cell cycle arrest at the G^1 phase. This combination also efficiently restrained the migration and invasion of breast cancer cells. The DTX or miRNA-142-3p alone can suppress malignant behavior and progression of breast cancer cells, but their combination elicits a synergistic effect that further enhances breast cancer inhibition. In summary, miRNA-142-3p transfection can be administered in conjunction with DTX therapy to enhance its cytotoxicity against breast cancer cells and prevent chemoresistance.

Introduction

Despite notable advancements in the treatment and diagnosis of breast cancer, it remains a prominent cause of death for women globally, contributing to as many as 40,000 annual fatalities.[1] A multitude of risk factors contribute to breast cancer development, including aging, reproductive history, family history of breast disease, environmental factors, and importantly, genetic predisposition.[2] Given the abnormal proliferation and metastasis of breast cancer cells, research has focused on comprehending the role of tumor-promoting factors in the progression of breast cancer and examining the expression of tumor-suppressing factors.[3-5] Aside from growth and migration, molecular pathways modulate the response of cancer cells to therapies, like chemotherapy, radiotherapy, and immunotherapy.[6,7] Uncovering molecular pathways holds the potential to disrupt breast cancer proliferation and invasion while improving therapy sensitivity. In the early stages, when cancer cells are still responsive and lack resistance, chemotherapy, particularly utilizing docetaxel (DTX) from the taxane family, is the preferred approach due to its minimally invasive nature.[8] The DTX exerts its anti-cancer effects by interfering with microtubules dynamics, preventing their deploymerization, and subsequent inhibition of mitosis through the addition of tubulin molecules.[9] However, widespread DTX usage has led to resistance mechanisms in cancer cells.[10] To address this, three strategies are under exploration, including employing nanoparticles for targeted DTX delivery, combining chemotherapy with other agents, and identifying pathways to restore

***Correspondence:**

Masoumeh Moradi Ozarlou. DVM, DVSc
Department of Pathobiology, Faculty of Veterinary Medicine, University of Tabriz, Tabriz, Iran
E-mail: ma.moradi@tabrizu.ac.ir

chemosensitivity.[11,12] MicroRNAs (miRNAs), short non-coding RNA molecules approximately 19 - 24 nucleotides long, regulate gene expression post-transcriptionally by binding to the 3' untranslated region of target mRNAs.[13] These miRNAs can also stimulate target gene expression, generating a recent surge in interest regarding their role in cancer therapy.[14] The irregular miRNA expression is linked to cancer-associated processes, like apoptosis, autophagy, migration, and differentiation.[15] Crucially, miRNAs modulate cancer cell responses to therapy, with an increase in tumor-promoting miRNAs and a decrease in tumor-suppressing miRNAs contributing to breast cancer malignancy and chemoresistance.[16,17] Initially identified as a tumor promoter in leukemia,[18] microRNA-142-3p has been revealed to also act as a tumor suppressor, hindering the growth, viability, and migration of cancer cells.[19,20] Thus, understanding the intricate role of this miRNA, a "double-edged sword" is crucial in the context of cancer. The study in focus explores the regulatory influence of microRNA-142-3p on breast cancer progression, examining *Bach1*, *HMGA2*, *SOX2*, *c-Myc*, *Octamer 4 (Oct4)*, and *Kruppel-like factor 4* (*KLF4)* as potential target genes. Additionally, it demonstrates the synergistic effect of miRNA-142-3p in enhancing DTX cytotoxicity against breast cancer cells. Ultimately, the research investigates the combined impact of miRNA-142-3p and DTX on breast cancer cell proliferation, apoptosis, and migration, aiming to elucidate its tumor-suppressing potential and role as a chemosensitizer.

Materials and Methods

Cell culture. The MDA-MB-468 human breast cancer cell line was grown in T-25 flasks using Gibco RPMI-1640 medium. The medium was supplemented with fetal bovine serum (FBS; Gibco, Carlsbad, USA), streptomycin (Sigma-Aldrich, St. Louis, USA), penicillin (Sigma-Aldrich), glutamine (Sigma-Aldrich), and sodium pyruvate (Sigma-Aldrich). The cells were maintained in a humidified incubator at 37.00 ˚C with 5.00% CO_2. During experiments, cells were sub-cultured upon reaching the logarithmic growth phase. The initial cell concentration was set at 5.00 × 10^5 cells *per* mL.

MicroRNA transfection. The MDA-MB-468 cells with the least miRNA-142-3p expression were selected for further experiments. The cells were prepared for miRNA-142-3p transfection upon reaching a density of 2.00 × 10^5 cells *per* well (5.00 × 10^5 cells were seeded in a 6-well plate and allowed to reach 60.00% confluency). Then, (1.00 mg mL^{-1}) polyethylenimine (Sigma-Aldrich) was mixed with miRNA at a 6:1 ratio. After a 15-min incubation, the mixture was added to the cells. Following the introduction of the cells and allowing them to grow until they achieved 60.00% coverage, the initial medium was replaced with OptiMEM (Gibco) medium, devoid of FBS or antibiotics. According to the established protocols, miRNA-142-3p (at concentrations of 1.00, 2.50, and 5.00 nM) was introduced to the cells using a jetPEI (Polyplus, Ismaning, Germany) transfection reagent. After incubating for 6 hr, the transfection medium was substituted with 2,000 µL of RPMI1640 medium (Gibco), being enhanced with a 10.00% concentration of FBS.

RNA isolation and cDNA generation. Total RNA isolation was performed using TRIzol reagent (Gene AII Biotechnology, Seoul, South Korea) following the manufacturer's instructions. To determine the RNA's quantity and purity, measurements were taken using a nanodrop spectrophotometer (Thermo Scientific, Waltham, USA). The absorbance at wavelengths of 280/260 nm and 260/230 nm was analyzed for this purpose. Subsequently, cDNA was synthesized from the isolated total RNA using the Exiqon kit (Exiqon, Copenhagen, Denmark). This cDNA was then utilized for the analysis of miRNA expression and target gene levels. The cDNA synthesis procedure was carried out using a RT-PCR system following established protocols.

Quantitative real-time polymerase chain reaction (qRT-PCR). The expression levels of miRNA-142-3p and its target genes were normalized to *U6* and *18s* internal reference genes (Table 1). SYBR GREEN technology was employed for performing qRT-PCR using a light cycler system. Custom-synthesized TaqMan primers from the Takapuzist Co. (Tehran, Iran) were utilized for the qRT-PCR reactions. The qRT-PCR procedure consisted of several steps. It commenced with an initial hold phase at 95.00 ˚C for 10 min, followed by 40 cycles. Each cycle comprised denaturation at 95.00 ˚C for 10 sec, annealing at 56.00 ˚C for 40 sec, and elongation at 72.00 ˚C for 20 sec. All tested genes indeed shared the same annealing temperature, being carefully selected based on primer design and optimization experiments to ensure specificity and efficiency.

Table 1. Primer sequences for genes utilized in quantitative real-time polymerase chain reaction.

Primers	Sequences
18S	F: 5′-CTACGTCCCTGCCCTTTGTACA-3′
	R: 5′-ACACTTCACCGGACCATTCAA-3′
Bach-1	F: 5′-TGCGATGTCACCATCTTTGT-3′
	R:5′-CCTGGCCTACGATTCTTGAG-3′
SOX2	F: 5′-ACATGTGAGGGCCGGACAGC-3′
	R:5′-TTGCGTGAGTGTGGATGGGATTGG-3′
Kruppel-like factor 4	F: 5′-ACCTTCTTCACCCCTAGAGC-3′
	R:5′-CCCAGTCACAGTGGTAAGGT-3′
c-Myc	F: 5′-CACATCAGCACAACTACGCA-3′
	R:5′-GCTCCAAGACGTTGTGTGT-3′
Octamer 4	F: 5′-GGCTCTTTGTCCACTTTGT-3′
	R:5′-GGCATGCATACACACAAACAC-3′
HMGA2	F: 5′-TGGGAGGAGCGAAATCTAAA-3′
	R:5′-TCCCTGGAGAAGAGCTACG-3′

MTT assay. The MTT assay was utilized to evaluate cell viability and ascertain the IC_{50} of DTX post-treatment. To evaluate the cytotoxic impact of miRNA-142-3p, different concentrations (1.00, 2.50, 5.00, and 7.00 nM) were utilized. For DTX, concentrations ranging from 0.001 to 100 nM and then, from 0.10 to 8.00 nM were applied. Finally, the cytotoxic effects of a combination of DTX and miRNA-142-3p were assessed. For the execution of MTT assay, cells were planted and treated in 96-well plates. Following a 24-hr incubation, the cells received 50.00 µL of MTT solution (2.00 mg mL^{-1}) and then incubated at 37.00 ˚C for 4 hr. After discarding the culture medium, 200 µL of dimethylsulfoxide was introduced into each well, and the plates were then incubated at 37.00 ˚C for 30 min. Ultimately, the plates were retrieved and read at a wavelength of 570 nm using an ELISA Reader (Tecan, Männedorf, Switzerland).

Wound healing assay. The approach to count migrated cells was chosen to provide a more quantitative assessment of migration in this specific context. After seeding the cells into 12-well plates, they were allowed to reach 70.00% confluency. Treatment with DTX, miRNA-142-3p, or their combination was then performed. Cell migration from the scratch edge to the scratch center was observed at 0 hr and 48 hr. Images were taken by an inverted light microscope (Model XDS-3; Optika, Bergamo, Italy) at 0 and 48 hr after transfection. The mobility of the cells from the edge of the gap area was determined using ImageJ Software (National Institutes of Health, Bethesda, USA).

Apoptotic assay using annexin V-fluorescein isothiocyanate/propidium iodide (FITC/PI) staining. This assay was utilized to evaluate the initiation of apoptosis. Cells were subjected to treatment with DTX, miRNA-142-3p, or a combination of both, followed by an additional incubation period at 37.00 ˚C for 24 hr. Subsequently, cells from each well were gathered and washed with phosphate buffered saline (PBS). Following that, the cells were re-suspended and exposed to 5.00 µL of annexin V-FITC conjugate and 5.00 µL of PI, with a subsequent 15-min incubation at room temperature. The assessment of apoptosis induction was then conducted using flow cytometry.

Cell cycle assay. This experiment aimed to investigate the potential of DTX, miRNA-142-3p, or their combination to induce cell cycle arrest. Cells were seeded in 6-well plates at a density of 2.00×10^5 cells *per* well and then incubated at 37.00 ˚C for 24 hr. After the incubation period, the cells were washed with PBS. Subsequently, a blend of 250 µL of trypsin and 250 µL of PBS was introduced into each well, and the cells underwent a 3-min incubation. Then, the cells were gathered from each well and moved into sterile micro-tubes (1.50 mL) for storage. The sterile micro-tubes underwent centrifugation at 1,200 rpm for 10 min. Subsequently, the cells were re-suspended in 500 µL of chilled PBS containing 20.00 mg mL^{-1} of PI and 5.00 µL of RNase A. The cell suspension was incubated at 37.00 ˚C for 30 min. Finally, cell cycle analysis was performed by flow cytometry (Partec, Munster, Germany).

Colony formation assay. This assay was utilized to evaluate the impact of DTX, miRNA-142-3p, or their combination on the capacity of cancer cells to form colonies. The cells were seeded in 6-well plates at a density of 5.00×10^3 cells *per* well and permitted to grow for one week. Subsequently, the cells underwent PBS washing, fixation in 5.00% paraformaldehyde for 10 min, and staining with crystal violet for 40 min.

Spheroid formation assay. The spheroid formation assay was included as a model to better mimic the three-dimensional structure of tumors *in vivo*, providing insights into the chemo-sensitizing effect of miRNA-142-3p in a more complex cellular arrangement. The cells were cultured in a serum-free medium (Gibco) supplemented with Matrigel (200 mg mL^{-1}) at a concentration of 1,000 cells *per* well. After 15 days, the formation of spheroids was evaluated using an inverted microscope. To measure the size of spheroid cells, ImageJ Software was utilized.

Statistical analysis. To predict potential target genes of miRNA-142-3p, several bioinformatic tools, including miRMap, miRbase, miRWALK, TargetScan, and miRANDA were employed. The gene expression comparison was conducted utilizing the 2-ΔΔCT method. The outcomes were presented as a mean ± standard deviation. Statistical significance among the control group, DTX treatment group, and miRNA-142-3p group was assessed through one-way ANOVA and two-way ANOVA. Statistical analysis was conducted using GraphPad Prism (version 7.0; GraphPad Software Inc., San Diego, USA), and significance was established with a threshold of *p*-values less than 0.05. Regarding the statistical analysis section, the Dunnett's Test and Tukey's Honestly Significant Difference Test as post-*hoc* tests were utilized following the analysis of variance to further explore the data. This choice was predicated on the specific nature of our data and analytical precision required for our study objectives.

Results

miRNA-142-3p exhibited the lowest expression levels in the MDA-MB-468 cell line, in comparison to the MCF-7, SKBR3, and MDA-MB-231 cell lines. The qRT-PCR outcomes displayed the miRNA-142-3p relative expression levels in the MDA-MB-231, MCF-7, SKBR3, and MDA-MB-468 cell lines as 0.014 ± 0.001, 0.008 ± 0.001, 0.007 ± 0.001, and 0.003 ± 0.001, respectively. Given that the MDA-MB-468 cell line displayed the lowest miRNA-142-3p expression level, these cells were chosen for additional experiments (Figs. 1 and 2).

Enhanced expression of miRNA-142-3p in MDA-MB-468 cells by mimic transfection. Fluorescence

microscopy confirmed successful transfection of the miRNA-142-3p mimic with an efficiency of approximately 60.00% (Fig. 2). The qRT-PCR findings revealed a dose-dependent increase in the expression level of miRNA-142-3p in the MDA-MB-468 cell line after transfection with various levels of the mimic. The relative expression of miRNA-142-3p in the control, negative control, and transfection groups with concentrations of 1.00, 2.50, and 5.00 nM was 1.00 ± 0.00, 1.00 ± 0.01, 2.20 ± 0.01, 4.10 ± 0.20, and 7.40 ± 0.30, respectively. A concentration of 5.00 nM was chosen for subsequent experiments since it led to a significant and statistically meaningful increase (p < 0.0001) in the expression of miRNA-142-3p compared to the control group (Figs. 3 and 4).

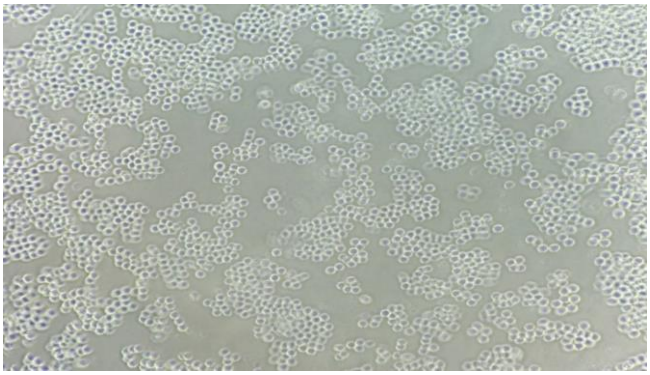

Fig. 1. Photomicrograph of MDA-MB-468 breast cancer cells (10× magnification).

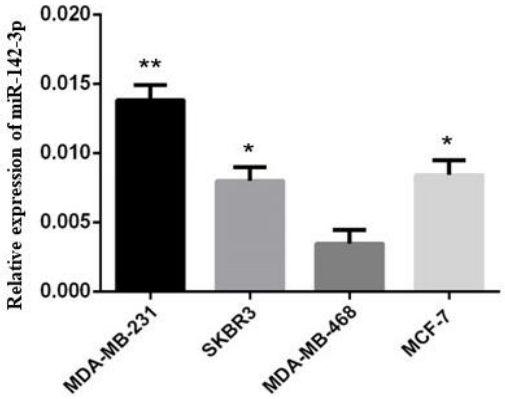

Fig. 2. Comparative examination of miRNA-142-3p expression in different breast cancer cell lines, including SKBR3, MDA-MB-231, MDA-MB-468, and MCF-7. $^{*}p < 0.05$, $^{**}p < 0.01$.

RNA quantity, quality, and purity using NanoDrop spectrophotometry. After transfecting the MDA-MB-468 cell line with miRNA-142-3p at concentrations of 1, 2.5, and 5 nM, the RNA was extracted. To assess the quantity, quality, and purity of the isolated RNA, Nanodrop Spectrophotometry was utilized.

Synergistic cytotoxic effect of miRNA-142-3p and DTX on MDA-MB-468 cells. The co-administration of DTX and miRNA-142-3p led to a considerable decrease in the IC_{50} value of DTX, resulting in 0.11 nM. As illustrated in Figure 5, this combination exhibited superior killing potential compared to the DTX alone at the same concentration. These results suggest that miRNA-142-3p increased the sensitivity of MDA-MB-468 cells to DTX, leading to a synergistic cytotoxic effect against breast cancer cells. To enhance our understanding of the relationship between DTX and miRNA-142-3p, the coefficient of drug interaction (CDI) at various levels of DTX was computed. When the CDI value is less than 1.00, it signifies a synergistic interaction, and if the CDI value is below 0.70, it suggests a notable synergistic effect. Conversely, CDI values equal to or exceeding 1.00 suggest additivity, whereas values surpassing 1.00 indicate antagonism. Throughout this study, CDI values consistently remained below 1.00 for all DTX concentrations, thereby confirming the presence of a synergistic interaction between miRNA-142-3p and DTX. This synergistic effect translated into a substantial enhancement of DTX cytotoxicity against MDA-MB-468 cells (Fig. 5).

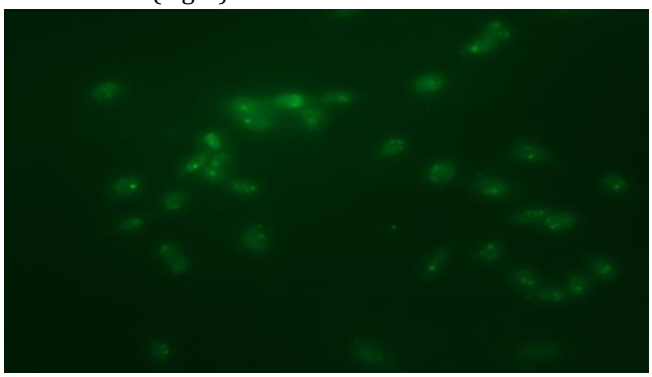

Fig. 3. Fluorescence microscopy image demonstrating the effective transfection of miRNA-142-3p into MDA-MB-468 cells, along with the detection of green fluorescent protein (GFP) protein signals. Cells expressing miRNA-142-3p appear green due to their interaction with GFP protein (40× magnification). The presence of GFP protein confirms successful transfection and expression of the microRNA sequence in the cells.

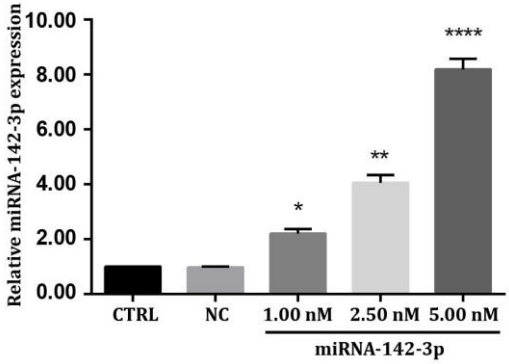

Fig. 4. The influence of transfection on miRNA-142-3p expression in MDA-MB-468 cells. The experiment was conducted in triplicate (n = 3), and the groups subjected to transfection showed significant changes in miRNA-142-3p expression compared to the control group ($^{*}p < 0.05$, $^{**}p < 0.01$, and $^{****}p < 0.0001$). CTRL: Control and NC: Negative Control.

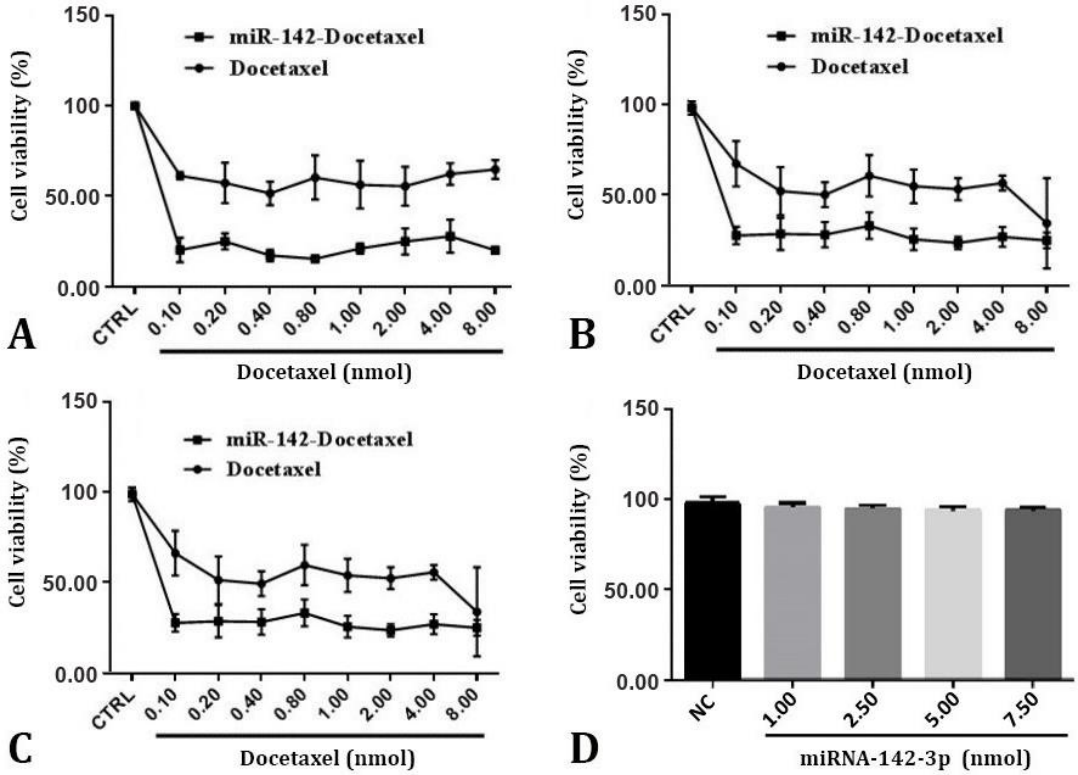

Fig. 5. Cytotoxicity analyses. **A)** The cell viability percentage in MCF-7 cells was evaluated following a 24-hr treatment with docetaxel (DTX) alone and the combined application of DTX and miRNA-142-3p; IC_{50} docetaxel: 2.67 nmol and IC_{50} miR-142-3p+ docetaxel: 0.07 nmol, **B)** The percentage of cell viability in MDA-MB-468 cells was determined after 24 hr of treatment with DTX alone and the combined application of DTX and miRNA-142-3p; IC_{50} docetaxel: 1.49 nmol and IC_{50} miR-142-3p+ docetaxel: 0.10 nmol, **C)** The percentage of cell viability in MDA-MB-231 cells was examined following a 24-hr treatment with DTX alone and the combined treatment of DTX and miRNA-142-3p; IC_{50} docetaxel: 1.33 nmol IC_{50} miR-142-3p+docetaxel: 0.11 mnol, and **D)** Assessment of the cytotoxic impact of miRNA-142-3p transfection alone on MDA-MB-468 cells.

No cytotoxic effect of miRNA-142-3p replacement on MDA-MB-468 cells. The investigation demonstrated that the transfection of miRNA-142-3p at a concentration of 5.00 nM did not induce a noteworthy cytotoxic effect on MDA-MB-468 cells in comparison with the control group. The viability of MDA-MB-468 cells upon miRNA-142-3p transfection in the negative control and transfected groups with concentrations of 1.00, 2.50, 5.00, and 7.00 nM remained relatively consistent, ranging from 99.00% to 96.00% (Fig. 5).

Co-administration of DTX and miRNA-142-3p significantly reduced expression of Bach-1 mRNA in MDA-MB-468 cell line. Following the transfection of MDA-MB-468 cells with a 5.00 nM miRNA-142-3p mimic and 0.11 nM of DTX, the assessment of Bach-1 mRNA expression was conducted through qRT-PCR. Importantly, the simultaneous application of miRNA-142-3p and DTX led to a substantial decrease in Bach-1 expression compared to the negative control group ($p < 0.0001$). The Bach-1 mRNA relative expression levels in the control group, DTX treatment group (1.33 nM), miRNA-142-3p transfection group (5.00 nM), and co-treatment group (0.11 nM DTX + 5.00 nM miRNA-142-3p) were 1.00 ± 0.00, 0.35 ± 0.10, 0.21 ± 0.04, and 0.01 ± 0.001, respectively (Fig. 6).

Combination therapy with miRNA-142-3p and DTX markedly reduced HMGA2 mRNA expression in MDA-MB-468 cell line. The joint application of miRNA-142-3p and DTX exhibited a notable reduction in HMGA2 mRNA levels compared to the control group ($p < 0.0001$). The qRT-PCR analysis demonstrated a considerable decrease in HMGA2 mRNA expression in the combination therapy group (0.30 ± 0.21) in comparison with the control group (1.00 ± 0.00), DTX treatment group (0.40 ± 0.23), and miRNA-142-3p transfection group (0.56 ± 0.25; Fig. 6).

miRNA-142-3p and DTX effectively down-regulated SOX2 mRNA expression in MDA-MB-468 cell line. The simultaneous use of DTX and miRNA-142-3p effectively lowered the levels of SOX2 mRNA in MDA-MB-468 cells in comparison with the control group ($p < 0.0001$). The relative expression of SOX2 mRNA in the control group (1.00 ± 0.00), DTX treatment group (0.40 ± 0.21), miRNA-142-3p transfection group (0.36 ± 0.23), and combined therapy group (0.09 ± 0.01) demonstrated the significant down-regulation of SOX2 mRNA in the combined therapy group (Fig. 6).

Concurrent utilization of DTX and miRNA-142-3p led to a substantial reduction in *c-Myc* expression in the MDA-MB-468 cell line. The outcomes revealed a notable reduction ($p < 0.0001$) in the mRNA expression level of *c-Myc* in the group treated with DTX and miRNA-142-3p in comparison with the negative control group. The *c-Myc* mRNA relative expression levels in the control group, DTX treatment group (1.33 nM), miRNA-142-3p transfection group (5.00 nM), and DTX (0.11 nM) and miRNA-142-3p (5.00 nM) group were 1.00 ± 0.00, 0.23 ± 0.05, 0.32 ± 0.07, and 0.004 ± 0.001, respectively (Fig. 6).

Combination of DTX and miRNA-142-3p led to a down-regulation in the expression level of *Oct4* mRNA in the MDA-MB-468 cell line. The findings revealed a significant reduction ($p < 0.0001$) in the expression of *Oct4* mRNA compared to the negative control group. The expression of *Oct4* mRNA was compared among different groups, including the control group, DTX treatment group (1.33 nM), miRNA-142-3p transfection group (5.00 nM), and combined treatment group of DTX (0.11 nM) and miRNA-142-3p (5.00 nM). The relative expression values were 1.00 ± 0.00, 1.10 ± 0.01, 0.36 ± 0.19, and 0.29 ± 0.18, respectively (Fig. 6).

Application of a combination of DTX and miRNA-142-3p resulted in a significant decrease in the expression of KLF4 in the MDA-MB-468 cell line. The results showed a notable reduction ($p < 0.0001$) in the expression of KLF4 mRNA in the group treated with DTX and miRNA-142-3p compared to the negative control group. The relative expression levels of KLF4 mRNA in the control group, DTX treatment group (1.33 nM), miRNA-142-3p transfection group (5.00 nM), and DTX (0.11 nM) and miRNA-142-3p (5.00 nM) group were 1.00 ± 0.00, 1.10 ± 0.08, 0.63 ± 0.21, and 0.52 ± 0.33, respectively (Fig. 6).

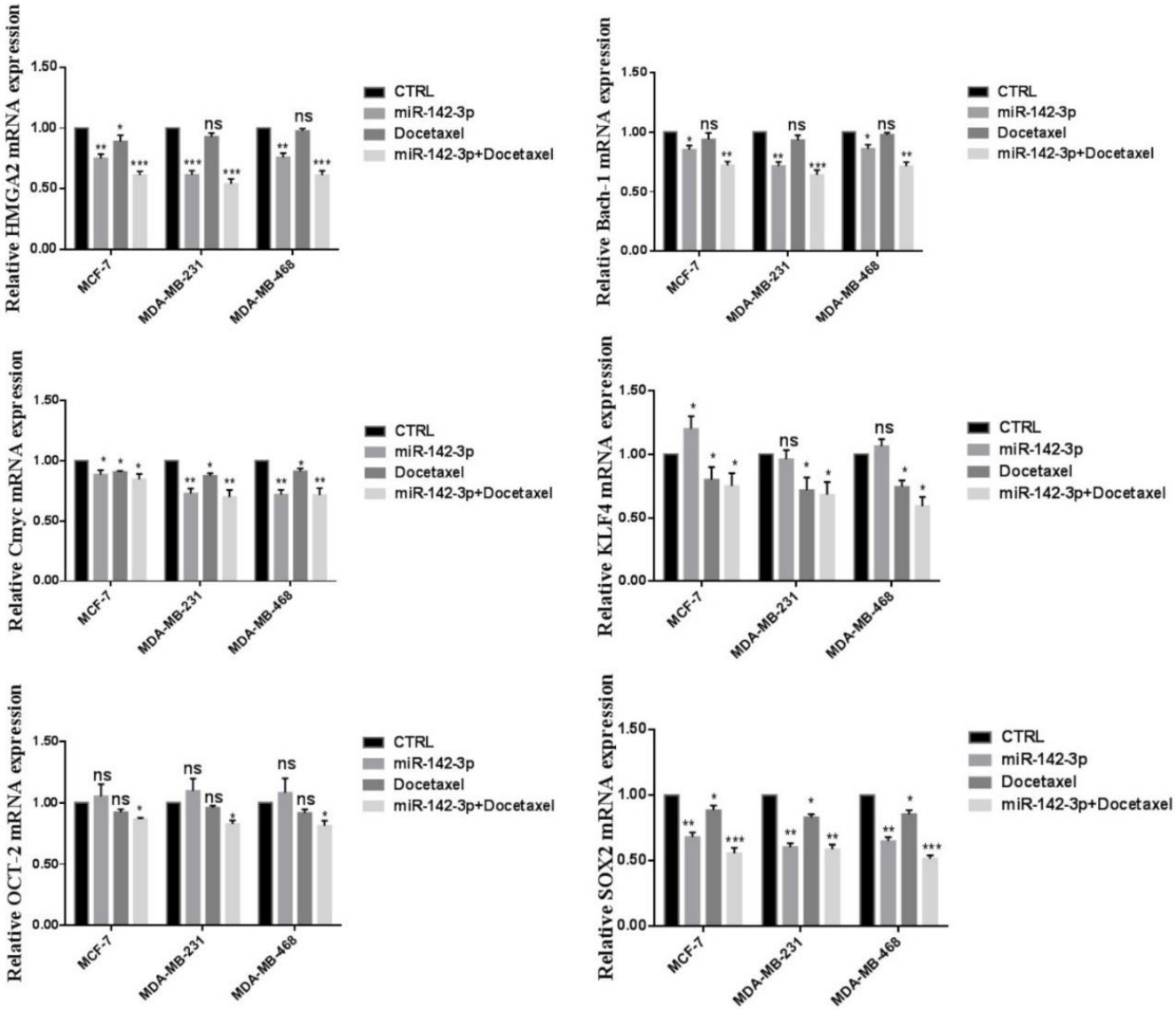

Fig. 6. Effects of docetaxel and miRNA-142-3p transfection on the expression levels of target genes ($^{*}p < 0.01$, $^{**}p < 0.001$, and $^{***}p < 0.0001$).

Joint application of DTX and miRNA-142-3p triggered apoptosis in the MDA-MB-468 cell line. To evaluate the level of apoptosis induction in different groups, flow cytometry and dual staining with annexin-V/PI were utilized. Through flow cytometry and employing annexin-V as an apoptosis marker, a significant rise in apoptosis induction was noted in the MDA-MB-468 cell line when exposed to the combination of DTX and miRNA-142-3p, compared to the negative control group ($p < 0.0001$). The levels of apoptosis induction in different groups, including the control group, miRNA transfection group (5.00 nM), DTX treatment group (1.33 nM), and combined treatment group of DTX (0.11 nM) and miRNA-142-3p (5.00 nM) were measured. The respective values were 0.40 ± 0.01, 2.30 ± 0.03, 3.10 ± 0.02, and 59.00 ± 0.00 (Fig. 7).

Concurrent application of DTX and miRNA-142-3p efficiently caused cell cycle arrest at the G_1 phase and elevated the cell population in the sub-G_1 phase. The findings showed that the treatment of the MDA-MB-468 cell line with DTX led to a significant rise in the number of cells in the G_0-G_1 phase, causing cell cycle arrest, in

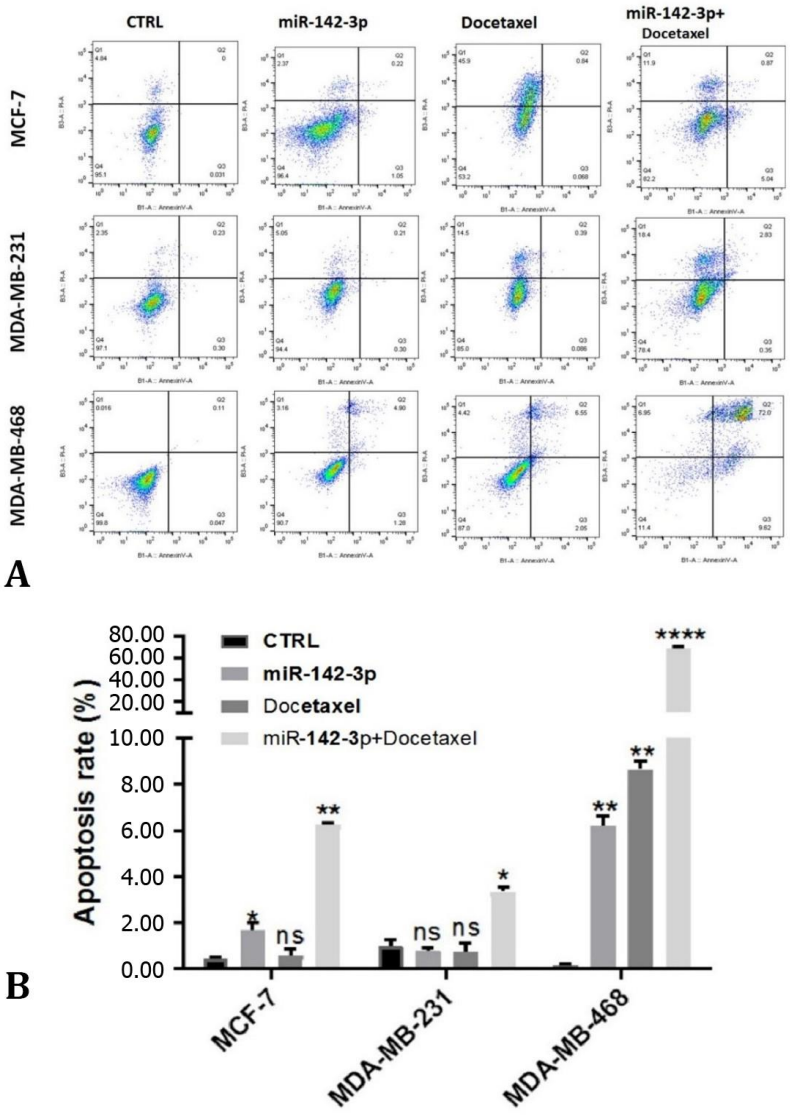

Fig. 7. Apoptosis and necrosis monitoring in breast cancer cells through annexin V-fluorescein isothiocyanate/propidium iodide staining. **A)** The investigation illustrates the reaction of three breast cancer cell lines, including MCF-7, MDA-MB-231, and MDA-MB-468, to combination therapy comprising docetaxel (DTX) and miRNA-142-3p. The MDA-MB-468 cells exhibit the most significant response to the combined therapy among the tested cell lines. In the lower-left quadrant, live cells are depicted, while the lower-right quadrant represents cells undergoing early apoptosis. The upper-left quadrant displays necrotic cells, and the upper-right quadrant portrays cells in the late stages of apoptosis; **B)** Apoptosis induction was noted in the MDA-MB-468, MDA-MB-231, and MCF-7 cell lines following treatment with DTX and miRNA-142-3p. Remarkably, MDA-MB-468 cells displayed increased sensitivity to the combined therapy ($^{*}p < 0.1$, $^{**}p < 0.01$, and $^{****}p < 0.0001$). CTRL: Control; ns: Non-significant.

comparison with the negative control group. In the miRNA-142-3p group, a minor increase in cell cycle arrest was observed. However, in the DTX and miRNA-142-3p group, a significant rise in the cell population within both the G_1 and sub-G_1 phases, which indicates apoptosis, was observed compared to the negative control group. In summary, following 24 hr of DTX treatment, there was a notable rise in the cell population in the G_1 phase and a decline in the cell population in the G_2/M phase. These findings highlight the inhibitory effect of DTX and its capability to induce cell cycle arrest. Moreover, there was a significant augmentation in the number of cells in the sub-G_1 phase, indicative of apoptotic cells, in the group subjected to miRNA-142-3p transfection. Although the observed increase in the DTX treatment group was less pronounced than that in the miRNA-142-3p group, it remained statistically significant. The noted elevation in the sub-G_1 phase in the miRNA-142-3p group implies the initiation of apoptosis in the MDA-MB-468 cell line. This effect is further amplified two-fold when combined with miRNA-142-3p, as depicted in Figure 8.

Combination of DTX and miRNA-142-3p significantly reduced colony formation in the MDA-MB-468 cell line. The results indicated a noteworthy decrease in colony formation in both the miRNA-142-3p transfection group and DTX treatment group compared to the control group ($p < 0.05$ and $p < 0.01$, respectively). Importantly, the combined application of DTX and miRNA-142-3p resulted in a substantial reduction in colony formation compared to both individual treatments ($p < 0.001$). In the combination group, there was a remarkable 80.00% reduction in colony formation compared to the negative control group. The colony formation numbers in the control group, miRNA-142-3p transfection group (5.00 nM), DTX treatment group (1.33 nM), and DTX (0.11 nM) and miRNA-142-3p (5.00 nM) group were 205.00 ± 5.00, 173.00 ± 3.00, 85.00 ± 5.00, and 49.00 ± 7.00, respectively (Fig. 9).

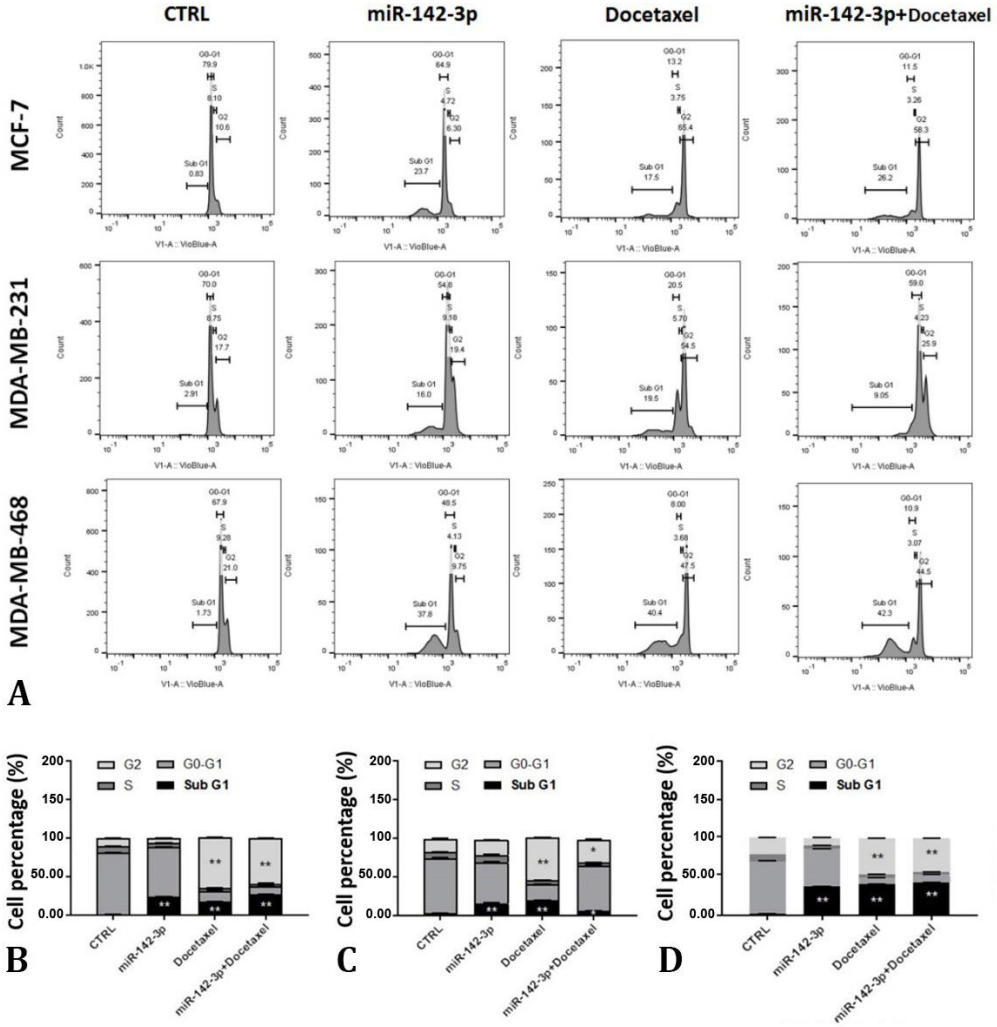

Fig. 8. Assessment of the cells population in the sub-G_1 phase using flow cytometry. **A)** The distribution of cell populations in various phases of the cell cycle; Among **B)** MCF-7, **C)** MDA-MB-231, and **D)** MDA-MB-468 breast cancer cell lines, MDA-MB-468 exhibited the greatest sensitivity to the combination therapy. CTRL: Control. ($^{*}p < 0.05$, $^{**}p < 0.01$).

Concurrent application of DTX and miRNA-142-3p proficiently hindered the migration of the MDA-MB-468 cell line. A wound healing assay was employed to assess the impact of DTX and miRNA-142-3p on cell migration. In the control group, cells migrated towards the scratch site, leading to an increase in cell numbers at the site. On the contrary, the groups subjected to DTX and miRNA-142-3p displayed a notable reduction in the number of migrated cells compared to the control group within 24 hr. Notably, in the combination group with DTX and miRNA-142-3p, this reduction reached an impressive 85.00%. The initial number of cells at the scratch site at 0 hr in the control group, miRNA-142-3p transfection group (5.00 nM), DTX treatment group (1.33 nM), and DTX (0.11 nM) and miRNA-142-3p (5.00 nM) group was 12.00 ± 5.00, 13.00 ± 2.00, 11.00 ± 2.00, and 12.00 ± 1.00, respectively. However, the number of migrated cells after 24 hr in these groups was 254.00 ± 12.00, 107.00 ± 4.00, 88.00 ± 4.00, and 34.00 ± 2.00, respectively (Fig. 10).

Combined DTX and miRNA-142-3p treatment substantially suppressed spheroid formation in breast cancer cell lines. To assess the impact of combined DTX and miRNA-142-3p therapy on cancer stem cell properties, spheroid formation was employed as an evaluation method. The results revealed a remarkable reduction in spheroid size in breast cancer cell lines following miRNA-142-3p transfection and DTX treatment in a three-dimensional *in vitro* assay (Fig. 11).

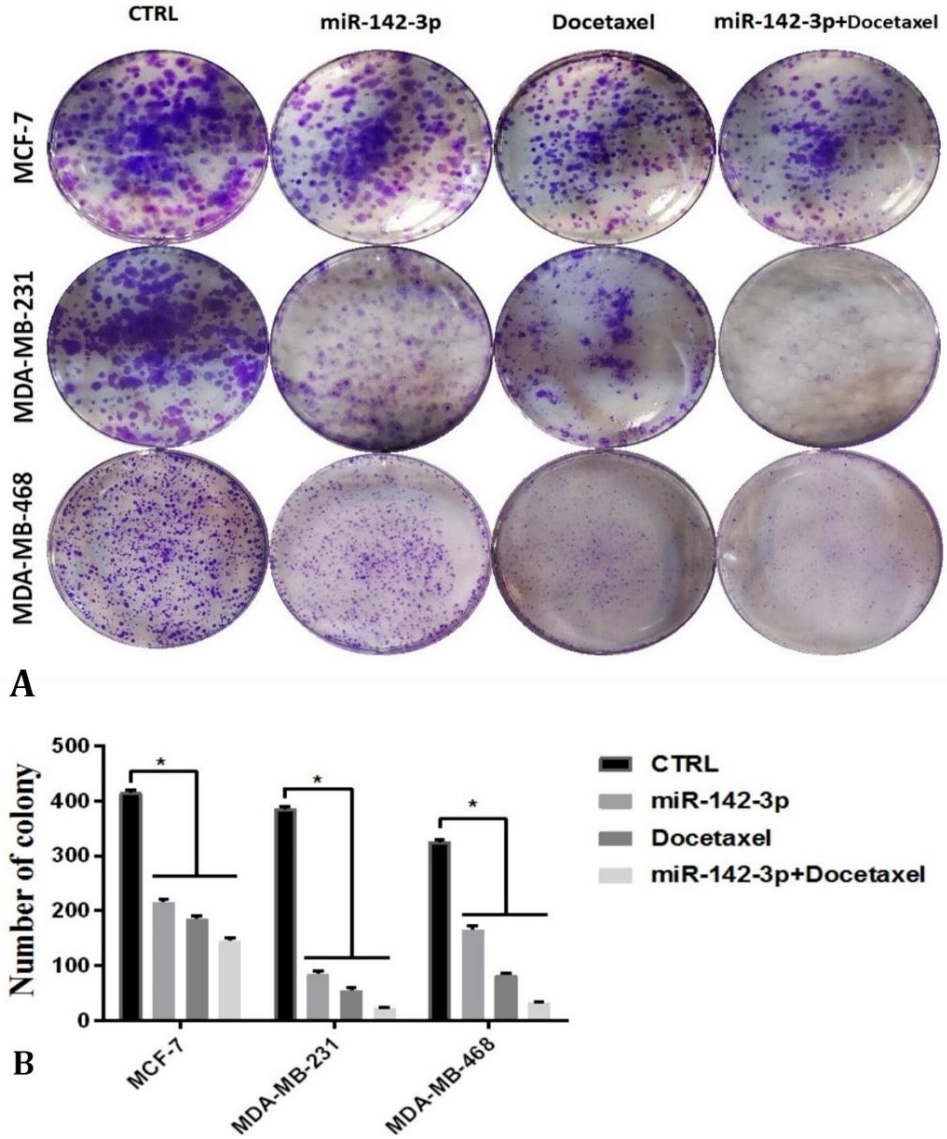

Fig. 9. Colony formation assays using crystal violet staining. **A)** Analyses demonstrate a significant reduction in colony formation upon treatment with miRNA-142-3p replacement and docetaxel (DTX), particularly in the MDA-MB-468 cell line; **B)** The formation of colonies was analyzed across the MDA-MB-231, MDA-MB-468, and MCF-7 cell lines after exposure to DTX, miRNA-142-3p replacement, or their combination for comparative assessment. CTRL: Control. ($^{*}p < 0.01$, $^{**}p < 0.001$, and $^{***}p < 0.0001$).

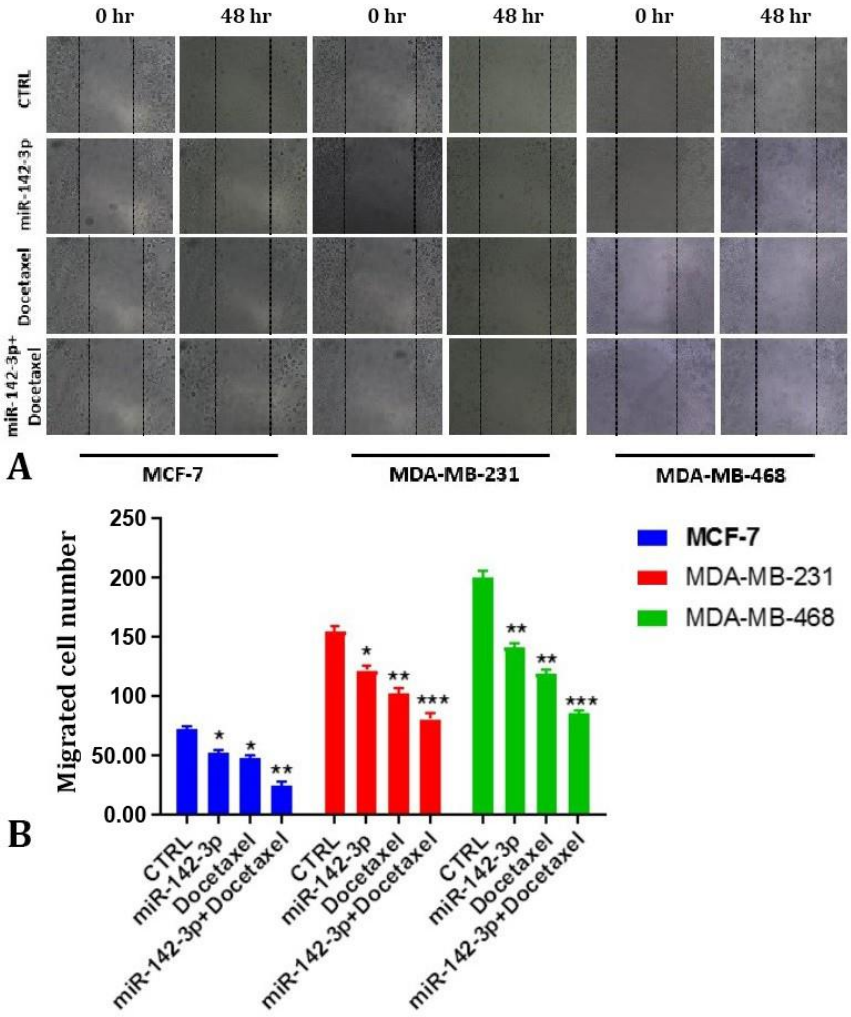

Fig. 10. Wound healing assay findings. **A)** The influence of miRNA-142-3p replacement, docetaxel (DTX; 1.33 nM), and their combination on the migration and invasion of breast cancer cell lines (MCF-7, MDA-MB-231, and MDA-MB-468); **B)** Assessing the comparative impact of DTX, miRNA-142-3p replacement, and their combination on the inhibition of migration in MCF-7, MDA-MB-468, and MDA-MB-231 cell lines ($^{*}p < 0.1$; $^{**}p < 0.01$; $^{***}p < 0.001$). CTRL: Control.

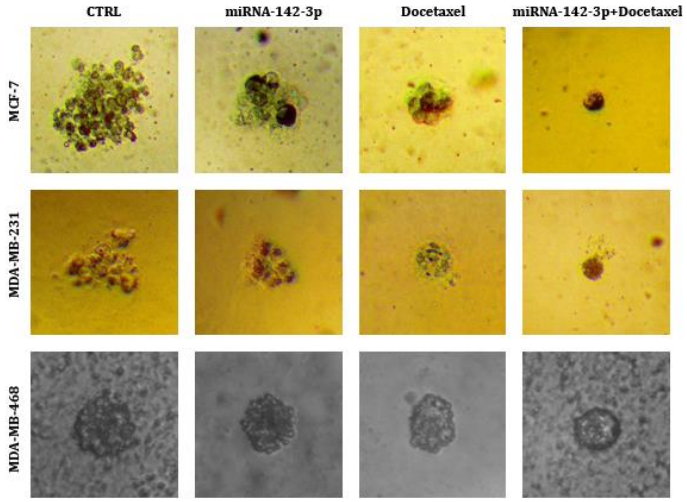

Fig. 11. Impact of docetaxel, miRNA-142-3p replacement, and their combination on the formation of spheroids in the MDA-MB-231, MDA-MB-468, and MCF-7 cell lines. CTRL: Control.

Discussion

MicroRNA-142-3p is a recently discovered miRNA, and significant efforts are underway to elucidate its precise role in cancer. As miRNAs can exhibit paradoxical functions in cancer, further investigations are needed to definitively establish whether miRNA-142-3p acts as a tumor suppressor or promoter. Nonetheless, recent findings predominantly support a tumor-suppressing role for miRNA-142-3p. Several studies have demonstrated its ability to simultaneously suppress both cancer cell proliferation and metastasis through up-regulation of Rac1 signaling. Consistent with its tumor-suppressing function, miRNA-142-3p expression is typically down-regulated during tumor progression.[21] The ability of miRNA-142-3p to inhibit cancer cell viability and invasion indicates its potential to enhance the chemosensitivity of cancer cells. In breast cancer cells, elevating miRNA-142-3p expression has been shown to suppress autophagy, thereby inducing chemosensitivity.[22] BTB and CNC homology 1 (Bach-1) is a heme-binding transcription factor playing a crucial role in regulating glucose metabolism and its incorporation into the tricarboxylic acid cycle. Notably, its down-regulation has been associated with enhanced sensitivity to mitochondrial inhibitors.[23] The Bach-1 expression is also a significant prognostic factor for breast cancer, with its up-regulation predicting a poorer prognosis and increased metastasis risk.[24] Consequently, there has been an increasing interest in exploring strategies to suppress Bach-1 expression for the treatment of breast cancer. Empirical evidence indicates that reducing Bach-1 expression significantly impedes proliferation and induces apoptosis in breast cancer cells. Moreover, inhibiting Bach-1 not only confines the migration of breast cancer cells but also accomplishes this by repressing the process of epithelial-to-mesenchymal transition (EMT).[25] Research investigations have unveiled that Bach-1 acts as a target for miRNAs in the context of breast cancer. MicroRNA-142-3p, a tumor-suppressing miRNA, acts by reducing Bach-1 expression at the mRNA level, leading to decreased viability and invasion.[26] Our research demonstrated that administration of DTX significantly diminishes Bach-1 expression in breast cancer cells. Additionally, miRNA-142-3p can also suppress Bach-1 expression. Notably, combining DTX and miRNA-142-3p therapy resulted in the greatest Bach-1 down-regulation, further enhancing DTX cytotoxicity against breast cancer cells. The HMGA2, recognized as a high-mobility group AT-hook 2, is another oncogenic factor found in breast cancer. It promotes metastasis by activating the Hippo signaling pathway and boosting the stability of YAP.[27] The heightened metastasis is linked to the over-expression of HMGA2, being attributed to its capacity to induce EMT.[28] Increased HMGA2 expression also promotes the survival of breast cancer cells and hinders apoptosis.[29] Non-coding RNAs serve as potential upstream regulators of HMGA2 in breast cancer. The long non-coding RNA LINC02163 facilitates HMGA2 expression by sequestering miRNA-511-3p, resulting in breast cancer proliferation and metastasis.[30] It is essential to target HMGA2 to improve the HMGA2 expression following DTX treatment compared to the control group. Although miRNA-142-3p contributed to the down-regulation of HMGA2, its impact was not as prominent as that of DTX. Similar to Bach-1, the combined administration chemosensitivity of breast cancer cells. Elevating the expression of miRNA-20a-5p has demonstrated a reduction in HMGA2 expression, thereby hindering breast cancer proliferation and invasion and rendering the cells more susceptible to apoptosis. In this investigation, we assessed how DTX and miRNA-142-3p influence HMGA2 expression in MDA-MB-468 cells. Our results indicated a notable reduction in of DTX and miRNA-142-3p resulted in the most significant decrease in HMGA2 expression, effectively suppressing the malignant behavior of breast cancer cells. Transcription factors known as SOX (sex-determining region Y-related HMG box) proteins, playing crucial roles in diverse developmental processes, are frequently observed to be elevated in cancer cells.[31] Upstream regulators manage the expression of SOX2 by binding to its promoter region.[32] Elevated levels of SOX2 contribute to increased metastasis of breast cancer cells to the brain through the activation of the protein kinase B (Akt) and beta-catenin signaling pathways.[33] Compounds with anti-tumor properties, such as bufalin, inhibit the progression and stemness of breast cancer by reducing the expression of SOX2. By suppressing SOX2 expression, miRNA-574-5p disrupts the proliferation and metastasis of breast cancer cells through the inhibition of EMT.[3] Breast cancer cells experienced a substantial reduction in SOX2 expression upon treatment with both DTX and miRNA-142-3p. Due to the synergistic effect between DTX and miRNA-142-3p, their combination achieves the most substantial reduction in SOX2 expression, effectively curbing tumor growth. Signaling through c-Myc, a recently identified therapeutic target in breast cancer, plays a pivotal role in tumor progression and resistance to chemotherapy.[34] Over-expression of this oncogene enhances pyruvate carboxylase expression, promoting breast cancer cell invasion.[35] Studies have provided evidence that caveolin-1 plays a role in inducing metabolic reprogramming in breast cancer. It improves patient survival by promoting the ubiquitination and subsequent proteasomal degradation of *c-Myc*.[36] Moreover, the signaling pathway involving *c-Myc* has a significant impact on how breast cancer cells respond to chemotherapy. Specifically, the M2 isoform of pyruvate kinase triggers *c-Myc*/survivin signaling, resulting in resistance to tamoxifen treatment.[37] On the contrary, inhibiting *c-Myc* increases the sensitivity of breast cancer cells to palbociclib.[38] Growing evidence suggests that

miRNAs can function as upstream regulators *of c-Myc* in cancer.[39] This trend is also observed in breast cancer cells, where DTX administration or miRNA-142-3p replacement leads to *c-Myc* down-regulation in MDA-MB-468 cells. The most significant reduction in *c-Myc* expression (>80.00%) is achieved by combining DTX and miRNA-142-3p. While DTX and miRNA-142-3p alone have a modest effect on *c-Myc* down-regulation, their synergistic combination effectively suppresses *c-Myc* expression and impedes breast cancer progression. Octamer 4 as a transcription factor linked to adverse clinical outcomes in cancer is a potential therapeutic target.[40] The Oct4 is involved in influencing the response of breast cancer cells to chemotherapy. Treatment of breast cancer cells with paclitaxel results in an up-regulation of hypoxia-inducible factor, subsequently triggering the expression of S100A10. This subsequently triggers Oct4 up-regulation, enhancing breast cancer stemness and rendering cells chemoresistant.[41] Additionally, Oct4 can promote Akt signaling, contributing to 5-fluorouracil resistance.[42,43] MicroRNAs in cancer can regulate *Oct4* expression. Tumor-suppressing miRNAs downregulate *Oct4* expression, hindering cancer progression.[44] The DTX treatment surprisingly induces *Oct4* expression, indicating a DTX-mediated *Oct4* up-regulation mechanism contributing to chemoresistance. However, miRNA-142-3p transfection significantly reduces *Oct4* expression. Combination therapy with DTX and miRNA-142-3p replacement produces a substantial decrease in *Oct4* expression compared to the control group, enhancing DTX cytotoxicity against breast cancer cells. Kruppel-like factor 4as another factor being down-regulated by miRNA-142-3p and DTX also plays a role in suppressing breast cancer progression. The outcomes of the wound healing assay unmistakably demonstrate that the joint application of DTX and miRNA-142-3p substantially hinders the migration of breast cancer cells.

Breast cancer cells have exhibited notable resilience, developing resistance to DTX despite its efficacy in eradicating cancer cells. Conversely, miRNAs have emerged as pivotal regulators influencing DTX sensitivity and resistance in breast cancer cells. Our study tested the hypothesis that down-regulation of miRNA-142-3p adversely impacts DTX's ability to eradicate breast cancer cells. Our findings support this hypothesis, as up-regulation of this tumor-suppressing miRNA effectively reduces the expression of oncogenes driving breast cancer progression, including *SOX2*, *Oct4*, *KLF4*, *HMGA2*, and *Bach-1*. Moreover, a combination of miRNA-142-3p and DTX significantly diminishes the expression of these genes, culminating in potent breast cancer suppression (Fig. 12). Additionally, this synergistic combination triggers apoptosis, inhibits cell cycle progression, and impedes breast cancer cells migration, further enhancing DTX's cytotoxic potential. Future investigations should prioritize the discovery of novel small molecules that could act as potential therapeutic targets for breast cancer treatment. Additionally, these studies should strive to augment the sensitivity of breast cancer cells to DTX.

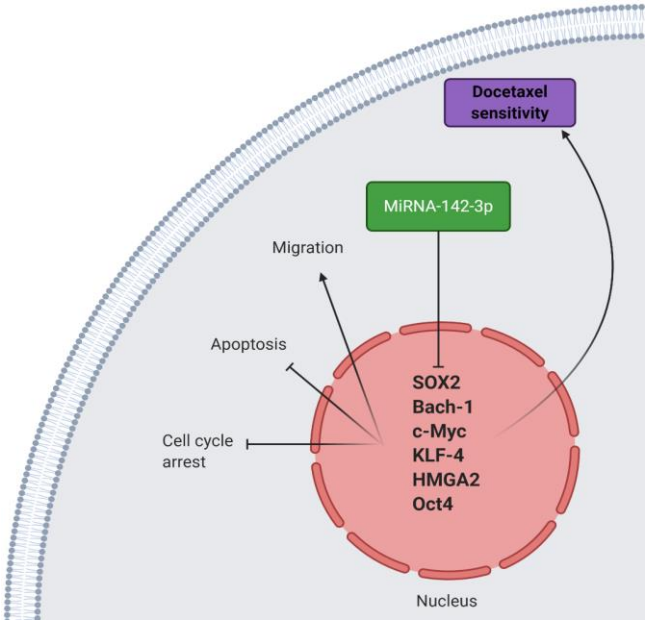

Fig. 12. Down-regulation of *SOX2*, *Bach-1*, *Kruppel-like factor 4* (*KLF-4)*, *c-Myc*, *HMGA2*, and *Octamer 4 (Oct4)* genes expression by miRNA-142-3p impedes breast cancer cells migration, induces apoptosis, and halts cell cycle progression, leading to enhanced docetaxel cytotoxicity.

Acknowledgments

The authors would like to extend their heartfelt appreciation to the Immunology Research Center at Tabriz University of Medical Sciences, Tabriz, Iran, for the invaluable support and provision of necessary facilities, greatly contributed to the successful completion of this research. The financial support for this work was also provided by this research facility. We acknowledge the oversight in explicitly mentioning our adherence to a code of ethics in the initial manuscript. We would like to clarify that all protocols used in this study were rigorously reviewed and approved by the Ethics Committee of Tabriz University of Medical Sciences, Tabriz, Iran, under the approval number of IR.TBZMED.REC.1396.982.

Conflict of interest

The authors declare that they have no known competing financial interests or personal relationships that could have appeared to influence the work reported in this paper.

References

1. Laborda-Illanes A, Sanchez-Alcoholado L, Dominguez-Recio ME, et al. Breast and gut microbiota action mechanisms in breast cancer pathogenesis and treatment. Cancers (Basel) 2020; 12(9): 2465. doi: 10.3390/cancers12092465.
2. Richardson AK, Walker LC, Cox B, et al. Breast cancer and cytomegalovirus. Clin Transl Oncol 2020; 22(4): 585-602.
3. Zhang KJ, Hu Y, Luo N, et al. miR‐574‐5p attenuates proliferation, migration and EMT in triple‐negative breast cancer cells by targeting BCL11A and SOX2 to inhibit the SKIL/TAZ/CTGF axis. Int J Oncol 2020; 56(5): 1240-1251.
4. Zhao B, Song X, Guan H. CircACAP2 promotes breast cancer proliferation and metastasis by targeting miR-29a/b-3p-COL5A1 axis. Life Sci 2020; 244: 117179. doi: 10.1016/j.lfs.2019.117179.
5. Zhou M, Dong M, Yang X, et al. The emerging roles and mechanism of m6a in breast cancer progression. Front Genet 2022; 13: 983564. doi: 10.3389/fgene. 2022.983564
6. 6. de Melo Gagliato D, Buzaid AC, Perez-Garcia J, et al. Immunotherapy in breast cancer: current practice and clinical challenges. BioDrugs 2020; 34(5): 611-623.
7. 7. Montemurro F, Nuzzolese I, Ponzone R. Neoadjuvant or adjuvant chemotherapy in early breast cancer? Expert Opin Pharmacother 2020; 21(9): 1071-1082.
8. Hashemi M, Zandieh MA, Talebi Y, et al. Paclitaxel and docetaxel resistance in prostate cancer: molecular mechanisms and possible therapeutic strategies. Biomed Pharmacother 2023; 160: 114392. doi: 10.1016/j.biopha.2023.114392.
9. Ahmed MB, Islam SU, Alghamdi AAA, et al. Phytochemicals as chemo-preventive agents and signaling molecule modulators: current role in cancer therapeutics and inflammation. Int J Mol Sci 2022; 23(24): 15765. doi: 10.3390/ijms232415765.
10. Sanchez-Hernandez ES, Ochoa PT, Suzuki T, et al. Glucocorticoid receptor regulates and interacts with LEDGF/p75 to promote docetaxel resistance in prostate cancer cells. Cells 2023; 12(16): 2046. doi: 10.3390/cells12162046.
11. Fan J, Zhang Z, Chen H, et al. *Zinc finger protein 831* promotes apoptosis and enhances chemosensitivity in breast cancer by acting as a novel transcriptional repressor targeting the *STAT3/Bcl2* signaling pathway. Genes Dis 2024; 11(1): 430-448.
12. Jurczyk M, Kasperczyk J, Wrześniok D, et al. Nanoparticles loaded with docetaxel and resveratrol as an advanced tool for cancer therapy. Biomedicines 2022; 10(5): 1187. doi: 10.3390/biomedicines 10051187.
13. Ashrafizadeh M, Ang HL, Moghadam ER, et al. MicroRNAs and their influence on the ZEB family: mechanistic aspects and therapeutic applications in cancer therapy. Biomolecules 2020; 10(7): 1040. doi: 10.3390/biom10071040.
14. Ashrafizadeh M, Zarrabi A, Hushmandi K, et al. Lung cancer cells and their sensitivity/resistance to cisplatin chemotherapy: role of microRNAs and upstream mediators. Cell Signal 2021; 78: 109871. doi: 10.1016/j.cellsig.2020.109871.
15. Shahverdi M, Hajiasgharzadeh K, Sorkhabi AD, et al. The regulatory role of autophagy-related miRNAs in lung cancer drug resistance. Biomed Pharmacother 2022; 148: 112735. doi: 10.1016/j.biopha. 2022.112735.
16. Fu R, Tong JS. miR-126 reduces trastuzumab resistance by targeting PIK3R2 and regulating AKT/mTOR pathway in breast cancer cells. J Cell Mol Med 2020; 24(13): 7600-7608.
17. Zeng J, Li G, Xia Y, et al. miR-204/COX5A axis contributes to invasion and chemotherapy resistance in estrogen receptor-positive breast cancers. Cancer Lett 2020; 492: 185-196.
18. Lv M, Zhang X, Jia H, et al. An oncogenic role of miR-142-3p in human T-cell acute lymphoblastic leukemia (T-ALL) by targeting glucocorticoid receptor-α and cAMP/PKA pathways. Leukemia 2012; 26(4): 769-777.
19. Chen HH, Huang WT, Yang LW, et al. The PTEN-AKT-mTOR/RICTOR pathway in nasal natural killer cell lymphoma is activated by miR-494-3p *via* PTEN but inhibited by miR-142-3p *via* RICTOR. Am J Pathol 2015; 185(5): 1487-1499.
20. Wu L, Cai C, Wang X, et al. MicroRNA-142-3p, a new regulator of RAC1, suppresses the migration and invasion of hepatocellular carcinoma cells. FEBS Lett 2011; 585(9): 1322-1330.
21. Li WQ, Zhao WC, Xin J, et al. MicroRNA-142-3p suppresses cell proliferation and migration in bladder cancer *via* Rac1. J Biol Regul Homeost Agents 2020; 34(1). doi: 10.23812/19-460-A.
22. Liang L, Fu J, Wang S, et al. MiR-142-3p enhances chemosensitivity of breast cancer cells and inhibits autophagy by targeting HMGB1. Acta Pharm Sin B 2020;10(6): 1036-1046.
23. Lee J, Yesilkanal AE, Wynne JP, et al. Effective breast cancer combination therapy targeting BACH1 and mitochondrial metabolism. Nature 2019; 568(7751): 254-258.
24. Ou X, Gao G, Bazhabayi M, et al. MALAT1 and BACH1 are prognostic biomarkers for triple-negative breast cancer. J Cancer Res Ther 2019; 15(7): 1597-1602.
25. Mansoori B, Mohammadi A, Asadzadeh Z, et al. HMGA2 and Bach-1 cooperate to promote breast cancer cell malignancy. J Cell Physiol 2019; 234(10): 17714-17726.
26. Mansoori B, Duijf PHG, Mohammadi A, et al. MiR-142-

3p targets HMGA2 and suppresses breast cancer malignancy. Life Sci 2021; 276: 119431. doi: 10.1016/j.lfs.2021.119431.
27. Xu J, Fang X, Long L, et al. HMGA2 promotes breast cancer metastasis by modulating Hippo-YAP signaling pathway. Cancer Biol Ther 2021; 22(1): 5-11.
28. Mansoori B, Duijf PHG, Mohammadi A, et al. Overexpression of HMGA2 in breast cancer promotes cell proliferation, migration, invasion and stemness. Expert Opin Ther Targets 2020; 24(3): 255-265.
29. Hashemi M, Rashidi M, Hushmandi K, et al. HMGA2 regulation by miRNAs in cancer: affecting cancer hallmarks and therapy response. Pharmacol Res 2023; 190: 106732. doi: 10.1016/j.phrs.2023.106732.
30. Qin C, Jin L, Li J, et al. Long noncoding RNA LINC02163 accelerates malignant tumor behaviors in breast cancer by regulating the MicroRNA-511-3p/HMGA2 axis. Oncol Res 2020; 28(5): 483-495.
31. Ashrafizadeh M, Taeb S, Hushmandi K, et al. Cancer and SOX proteins: new insight into their role in ovarian cancer progression/inhibition. Pharmacol Res 2020; 161: 105159. doi: 10.1016/j.phrs.2020.105159.
32. Liang S, Takahashi H, Hirose T, et al. NONO is a negative regulator of *SOX2* promoter. Cancer Genomics Proteomics 2020; 17(4): 359-367.
33. Xiao W, Zheng S, Xie X, et al. *SOX2* promotes brain metastasis of breast cancer by upregulating the expression of FSCN1 and HBEGF. Mol Ther Oncolytics 2020; 17: 118-129.
34. Gao FY, Li XT, Xu K, et al. c-MYC mediates the crosstalk between breast cancer cells and tumor microenvironment. Cell Commun Signal 2023; 21(1): 28. doi: 10.1186/s12964-023-01043-1.
35. Lao-On U, Rojvirat P, Chansongkrow P, et al. c-Myc directly targets an over-expression of pyruvate carboxylase in highly invasive breast cancer. Biochim Biophys Acta Mol Basis Dis 2020; 1866(3): 165656. doi: 10.1016/j.bbadis.2019.165656.
36. Wang S, Wang N, Zheng Y, et al. Caveolin-1 inhibits breast cancer stem cells *via* c-Myc-mediated metabolic reprogramming. Cell Death Dis 2020; 11(6): 450. doi: 10.1038/s41419-020-2667-x.
37. Yu P, Li AX, Chen XS, et al. PKM2–c-Myc–Survivin cascade regulates the cell proliferation, migration, and tamoxifen resistance in breast cancer. Front Pharmacol 2020; 11: 550469. doi: 10.3389/fphar.2020.550469.
38. Ji W, Zhang W, Wang X, et al. c-myc regulates the sensitivity of breast cancer cells to palbociclib *via* c-myc/miR-29b-3p/CDK6 axis. Cell Death Dis 2020; 11(9): 760. doi: 10.1038/s41419-020-02980-2.
39. Liu N, Steer CJ, Song G. MicroRNA-206 enhances antitumor immunity by disrupting the communication between malignant hepatocytes and regulatory T cells in c-Myc mice. Hepatology 2022; 76(1): 32-47.
40. Jahangiri R, Mosaffa F, EmamiRazavi A, et al. Increased expression of gankyrin and stemness factor Oct-4 are associated with unfavorable clinical outcomes and poor benefit of tamoxifen in breast carcinoma patients. Pathol Oncol Res 2020; 26(3): 1921-1934.
41. Lu X, Yang F, Chen D, et al. Quercetin reverses docetaxel resistance in prostate cancer *via* androgen receptor and PI3K/Akt signaling pathways. Int J Biol Sci 2020;16(7): 1121-1134.
42. Dorna D, Paluszczak J. Targeting cancer stem cells as a strategy for reducing chemotherapy resistance in head and neck cancers. J Cancer Res Clin Oncol 2023; 149(14): 13417-13435.
43. Yao X, Tu Y, Xu Y, et al. Endoplasmic reticulum stress confers 5-fluorouracil resistance in breast cancer cell *via* the GRP78/OCT4/lncRNA MIAT/AKT pathway. Am J Cancer Res 2020; 10(3): 838-855.
44. Chang YC, Yang YF, Chiou J, et al. Nonenzymatic function of Aldolase A downregulates miR-145 to promote the Oct4/DUSP4/TRAF4 axis and the acquisition of lung cancer stemness. Cell Death Dis 2020; 11(3):195. doi: 10.1038/s41419-020-2387-2.